

# Jitter Self-Compton Process: GeV Emission of GRB 100728A

Jirong Mao

*Korea Astronomy and Space Science Institute, 776, Daedeokdae-ro, Yuseong-gu, Daejeon  
305-348, Republic of Korea*

*Yunnan Observatory, Chinese Academy of Sciences, Kunming, Yunnan Province 650011,  
China*

*Key Laboratory for the Structure and Evolution of Celestial Objects, Chinese Academy of  
Sciences, Kunming, China*

jirongmao@kasi.re.kr

Jiancheng Wang

*Yunnan Observatory, Chinese Academy of Sciences, Kunming, Yunnan Province, 650011,  
China*

*Key Laboratory for the Structure and Evolution of Celestial Objects, Chinese Academy of  
Sciences, Kunming, China*

## ABSTRACT

Jitter radiation, the emission of relativistic electrons in a random and small-scale magnetic field, has been applied to explain the gamma-ray burst (GRB) prompt emission. The seed photons produced from jitter radiation can be scattered by thermal/nonthermal electrons to the high-energy bands. This mechanism is called jitter self-Compton (JSC) radiation. GRB 100728A, which was simultaneously observed by the *Swift* and *Fermi*, is a great example to constrain the physical processes of jitter and JSC. In our work, we utilize jitter/JSC radiation to reproduce the multiwavelength spectrum of GRB 100728A. In particular, due to JSC radiation, the powerful emission above the GeV band is the result of those jitter photons in X-ray band scattered by the relativistic electrons with a mixed thermal-nonthermal energy distribution. We also combine the geometric effect of microemitters to the radiation mechanism, such that the “jet-in-jet” scenario is considered. The observed GRB duration is the result of summing up all of the contributions from those microemitters in the bulk jet.

*Subject headings:* acceleration of particles — gamma ray burst: individual (GRB 100728A) — gamma rays: general — radiation mechanisms: non-thermal — shock waves — turbulence

## 1. Introduction

Gamma-ray bursts (GRBs) are objects emitting high-energy photons. One detection of a GeV photon from GRB 940217 was reported 17 years ago (Hurley et al. 1994). Compared with the previous research, recently, with Large Area Telescope (LAT) on board the *Fermi* satellite, we have more observational cases for the study of GRB high-energy emission above 100 MeV. It is more important that the published multi-wavelength data of GRB 090510 and GRB 100728A have been provided by the simultaneous observations of the *Swift* and *Fermi* (De Pasquale et al. 2010; Abdo et al. 2011). Some radiation models can be constrained by these simultaneous data.

It is hard to apply the simple synchrotron model for the explanation of high-energy emission from GRB 941017 (González et al. 2003). In general, the photons produced by synchrotron radiation can be scattered by the relativistic electrons. Therefore, an inverse Compton process or synchrotron self-Compton (SSC) process is proposed naturally to explain the GRB emission above the GeV band (Mészáros et al. 1993; Dermer et al. 2000; Wang et al. 2001; Zhang & Mészáros 2001; Granot & Guetta 2003; Fan et al. 2008; Zou et al. 2009; Corsi et al. 2010). In particular, the possibility was suggested that the photons from X-ray flares can be scattered to the GeV band by those relativistic electrons (Wang et al. 2006; Galli & Guetta 2008).

From a theoretical point of view, Mészáros et al. (1994) first mentioned the physics of turbulent field growth for the study of GRB radiation. Narayan & Kumar (2009) proposed one model in which the GRB radiating fluid is relativistically turbulent. This turbulent process, plus the inverse Compton mechanism, was applied to the study of radiation in GRB 080319B (Kumar & Narayan 2009). In the turbulent fluid, the random and small emitters can produce short-time variabilities, indicating many pulses shown in the GRB prompt light curve (Lyutikov 2006; Lazar et al. 2009). It is worth noting the key point of this “jet-in-jet” model: these microemitters within the bulk jet of GRB explosion also have a jet structure.

The turbulent scenario mentioned above is consistent with the principle of jitter mechanism. Jitter radiation, which is the emission of relativistic electrons in a random and small-scale magnetic field, has been applied to GRB research (Medvedev 2000, 2006). The random and small-scale magnetic field can be generated by Weibel instability (Medvedev & Loeb 1999). Alternatively, we propose that the turbulent cascade process can also produce the random and small-scale magnetic field (Mao & Wang 2007, 2011). As the magnetic field may have a sub-Larmor length scale, the jitter radiation in this sub-Larmor scale magnetic field was fully studied by Medvedev & Spitkovsky (2009) and Medvedev et al. (2011). The small-scale turbulent dynamo with large Reynolds numbers at a saturated state in a fluid flow was simulated by Schekochihin et al. (2004). The simulation identified a power-law

turbulent energy spectrum. In our model, the complicated jitter radiation is simplified as a one-dimensional case to study GRB prompt emission. From this specified jitter radiation, the spectral index of a single electron is directly related to the turbulent energy spectrum.

In general, the electron energy distribution is assumed to be a power law. However, in the turbulent framework, stochastic acceleration may be effective. Schlickeiser (1989a,b) found a Maxwellian energy distribution of electrons. A similar quasithermal stationary solution of stochastic acceleration was given by Katarzyński et al. (2006). In a turbulent magnetic field, the stochastic acceleration of ultrarelativistic electrons was also discussed by Stawarz & Petrosian (2008). With the Maxwellian electron energy distribution, the radiative spectrum and light curve of GRB afterglow were calculated by Giannios & Spitkovsky (2009).

As suggested by Kirk & Reville (2010), if the jitter photons in the keV band are scattered by the relativistic electrons, the final output emission will be in the GeV band. In this work, we attempt to calculate the inverse Compton scattering of jitter radiation. Similar to the SSC mechanism, this process can be called as “jitter self-Compton” (JSC) mechanism. At present, we have only two published data sets of GRBs (GRB 090510 and GRB 100728A), which were obtained by the simultaneous observations from *Swift* and *Fermi*. In particular, the extremely powerful X-ray flares and GeV emission of GRB 100728A were observed by *Swift*/X-ray telescope (XRT) and *Fermi*/LAT, respectively. Thus, the case of GRB 100728A provides us an excellent chance to study the powerful GeV emission and the link between keV emission and GeV emission in the GRB multiwavelength spectrum. In this work, the multiwavelength spectral result of GRB 100728A is especially precious to constrain our theoretical model of jitter/JSC radiation. Furthermore, from the clues of Lyutikov (2006) and Lazar et al. (2009), we expect that the observed gross emission from a bulk jet launched by GRB explosion might be related to the emissions from the small-scale emitters with the minijet structure. Therefore, in this paper, we stress the following issues. (1) To prove the jitter/JSC mechanism, which may work for GRB prompt/GeV-band emission, we use the multiwavelength spectrum of GRB 100728A (Abdo et al. 2011) as an example. (2) In our former research (Mao & Wang 2011), jitter has been identified as the possible radiation mechanism for the GRB prompt emission, and turbulence is the dominant dynamic process. Here, some further, detailed calculations are required to fit the observational data of GRB 100728A. (3) The JSC mechanism can be examined because the multiwavelength spectrum of GRB 100728A has been given. (4) The final JSC result is dependent on the electron energy distribution. (5) Since the turbulent dynamics has been applied in Mao & Wang (2011), as a consequent step, the link between the microemitters with the minijet structure and the emission of the GRB bulk jet should be considered. (6) As calculated by Mao & Wang (2011), the cooling timescale of relativistic electrons has a typical value of about  $10^{-8}$  s. The observed duration of GRB prompt emission is much longer than the cooling timescale, so

further explanations are required.

In Section 2.1, we first briefly describe our specific case of jitter radiation and then fully present the JSC process. In Section 2.2, we illustrate the “jet-in-jet” scenario and link the minijets to the bulk jet structure. In Section 2.3, combined with the “jet-in-jet” effect, our jitter/JSC model can reproduce the multiwavelength spectral properties of GRB 100728A. In particular, we focus on the GeV emission detected by *Fermi*/LAT and the JSC process. The observed GRB duration can also be estimated. Conclusions and discussion are given in Section 3.

## 2. JSC Process and Application of GRB 100728A

There are two important issues concerning the following jitter/JSC calculations: (1) Because stochastic acceleration is one of the key points in this work, the Maxwellian energy distribution of relativistic electrons should be applied in the calculation. (2) The gross temporal profile of GRB prompt emission can be the result of superimposing from a large amount of short-timescale pulses.

### 2.1. JSC Process

Jitter radiation is the emission of relativistic electrons in a random and small-scale magnetic field. In a one-dimensional case, the simplified formulas of jitter radiation have been derived (Mao & Wang 2007, 2011). We also propose that a random and small-scale magnetic field can be produced by turbulence. The radiative intensity of a single electron has a power-law shape, and the spectral index is related to the energy spectrum of turbulent flow. Here, we write the radiative intensity in the unit of  $\text{erg s}^{-1} \text{Hz}^{-1}$  as

$$I_{\nu,\text{jitter}} = \frac{8e^4}{3m_e^2c^3} \nu^{-(\zeta_p-1)}, \quad (1)$$

where  $\zeta_p$  is the index determined by the turbulent energy cascade and  $c$  is the light speed. In this simplified case, we note that the jitter radiation of a single electron is not related to the electron Lorentz factor  $\gamma$ . The radiative flux of a single electron can be simply estimated by  $I_{\nu,\text{jitter}}ct_{\text{cool}}$ , where  $t_{\text{cool}}$  is the radiative cooling timescale of relativistic electrons.

The process of inverse Compton scattering can be calculated by a standard recipe (Rybicki & Lightman 1979). The SSC radiation has been fully discussed as well (e.g., Chiang & Dermer 1999). In principle, our JSC process can follow the same SSC calculation procedure. The

emission flux density in the unit of  $\text{erg s}^{-1} \text{cm}^{-3} \text{Hz}^{-1}$  is

$$j_{\nu,\text{jsc}} = 8\pi r_0^2 c h \int_{\nu_{0,\text{min}}}^{\nu_{0,\text{max}}} \int_{\gamma_{\text{min}}}^{\gamma_{\text{max}}} N(\gamma) f(\nu/4\gamma^2\nu_0) n_{\text{ph}}(\nu_0) d\nu_0 d\gamma, \quad (2)$$

where  $f(x) = x + 2x^2 \ln x + x^2 - 2x^3$  for  $0 < x < 1$ ,  $f(x) = 0$  for  $x > 1$ , and  $x \equiv \nu/4\gamma^2\nu_0$ . The Thomson scattering section is  $\sigma_T = 8\pi r_0^2/3 = 6.65 \times 10^{-25} \text{cm}^2$ .  $n_{\text{ph}}(\nu_0)$  is the number density of seed photons, and it can be easily calculated from the jitter radiation as  $n_{\text{ph}}(\nu_0) = t_{\text{cool}} \int (I_{\nu,\text{jitter}}/h\nu) d\nu \int N(\gamma) d\gamma$ ,  $N(\gamma)$  is the electron energy distribution.  $\nu_{0,\text{min}}$  and  $\nu_{0,\text{max}}$  are the lower and upper limits of jitter radiative frequency, respectively.  $\gamma_{\text{min}}$  and  $\gamma_{\text{max}}$  are the lower and upper limits of relativistic electron Lorentz factor, respectively.

In general, the electron energy distribution can be given as a power law:  $N(\gamma) \propto \gamma^{-p}$ , where  $p = 2.2$ . In this paper, the turbulent process is one of the vital points for GRB prompt emission and particle acceleration. As mentioned in Section 1, due to stochastic acceleration, the Maxwellian function of electron energy distribution can be obtained. Here, we follow the description of electron energy distribution given by Giannios & Spitkovsky (2009) as

$$N(\gamma) = C\gamma^2 \exp(-\gamma/\Theta)/2\Theta^3 \quad (3)$$

for  $\gamma \leq \gamma_{\text{nth}}$  and

$$N(\gamma) = C[\gamma^2 \exp(-\gamma/\Theta)/2\Theta^3](\gamma/\gamma_{\text{nth}})^{-p} \quad (4)$$

for  $\gamma > \gamma_{\text{nth}}$ , where  $C$  is the normalization constant,  $\gamma_{\text{nth}}$  is the connection number between the Maxwellian and power law components, and  $\Theta = kT/m_e c^2$  is a characteristic temperature. We use this mixed thermal-nonthermal electron energy distribution to calculate jitter/JSC radiation. In the case of  $\gamma_{\text{min}} = \gamma_{\text{nth}}$ , the mixed thermal-nonthermal distribution is reduced to a pure power-law distribution.

## 2.2. Jet-in-jet Scenario

We draw a sketch to illustrate the “jet-in-jet” scenario, as shown in Figure 1. The term of “jet-in-jet” means that those microemitters radiating as minijets are within the bulk jet. Giannios et al. (2010) proposed an “off-axis” parameter  $\alpha$  defined by  $\theta_j = \alpha/\Gamma_j$ , where  $\Gamma_j$  is the bulk Lorentz factor of the jet launched by GRB and  $\theta_j$  is the related view angle. The gross Lorentz factor can be derived as  $\Gamma = 2\Gamma_j\Gamma_e/\alpha^2$ , and  $\Gamma_e$  is the Lorentz factor of the minijet. In our work, because these minijets point randomly in the bulk jet but all of them move with a general turbulent velocity, we use  $\Gamma_e \sim \Gamma_t$ , and  $\Gamma_t = 10$  is the turbulent Lorentz factor adopted by Narayan & Kumar (2009).

The possibility of observing these minijets can be estimated by  $P = 2\pi \int_0^\theta \sin\theta' d\theta' / 4\pi = \theta^2/4 = 1/4\Gamma^2$ . The observed flux is  $\nu f(\nu) = P\delta^{2+w}\nu' f(\nu')$ , where  $\nu' f(\nu')$  is the flux calculated in the GRB shell frame,  $w$  is the spectral index, and  $\delta$  is the Doppler factor. Here, we take  $w = 1$  and  $\delta \sim \Gamma$ .

In the GRB shell frame, the microemitter has the length scale of  $l_s = \gamma ct_{\text{cool}}$ . The total number of microemitters within the fireball shell is  $n = 4\pi R^2 \delta_s / l_s^3$ , where  $R \sim 10^{13}$  cm is the fireball radius and  $\delta_s = ct_{\text{cool}}$  is the thick of the shell. The length scale of the turbulent eddy is  $l_{\text{eddy}} \sim R/\Gamma$  (Narayan & Kumar 2009). We can define a dimensionless scale as  $n_l = l_{\text{eddy}}/l_s$ . Therefore, we sum up the contributions of the microemitters within the turbulent eddy and obtain the total observed duration of GRB emission as  $T = n_l n P \Gamma t_{\text{cool}}$ . We calculate these parameters in the next subsection.

### 2.3. High-Energy Emission of GRB 100728A

To quantitatively study the jitter/JSC process, we use GRB 100728A as an example. GRB 100728A was detected by *Swift*/XRT (0.3-10 keV), *Swift*/Burst Alert Telescope (BAT, 15-150 keV), *Fermi*/Gamma-ray Burst Monitor (10-1000 keV), and *Fermi*/LAT (above 100 MeV). The spectrum observed by the BAT and XRT can be well fitted by the Band function with spectral index  $\alpha = -1.06$  and  $\beta = -2.24$  and peak energy  $E_{\text{pk}} = 1.0$  keV (Abdo et al. 2011). This spectral function can be extrapolated to the GeV band. The X-ray emission was dominated by a series of bright X-ray flares with a maximum rate above 800 *counts s*<sup>-1</sup>. In the time interval of strong X-ray flare activity, a significant GeV emission was detected by *Fermi*/LAT. We take these observational data from Abdo et al. (2011) and plot them in Figure 2.

We perform the jitter/JSC calculations to reproduce the multiwavelength spectrum of GRB 100728A and also plot the results in Figure 2. We adopt  $\Gamma_j = 100$ ,  $\Gamma_t = 10$ , and “off-axis” parameter  $\alpha = 1$ .  $C = 1.7 \times 10^{10}$  cm<sup>-3</sup> is the value of the electron number density in the relativistic shock. Using the spectral index determined by the energy spectrum of turbulent flow, we can reproduce X-ray and prompt emissions of GRB 100728A through the jitter mechanism. Here,  $\zeta_p = 2.24$  is in the theoretical range of the turbulent energy cascade (She & Leveque 1994).

With the electron energy distribution presented by Equations (3) and (4), fixing  $\gamma_{\text{min}} = 100$ ,  $\gamma_{\text{max}} = 10^6$ , and  $\gamma_{\text{nth}} = 10^3$ , we can obtain the JSC result. We adopt  $\Theta = 200$ , which corresponds to the plasma temperature above  $10^{12}$  K. The radiative cooling timescale  $t_{\text{cool}}$  is given as  $2.2 \times 10^{-8}$  s (see the calculation below). The frequency  $\nu_{0,\text{max}} = 4.2$  keV is also

considered. It indicates that X-ray emission, which is dominated by X-ray flares in this case, provides enough target photons for the relativistic electron scattering. For comparison, using a pure power-law electron energy distribution ( $\gamma_{\min} = \gamma_{\text{nth}} = 10^3$ ), we also calculate the JSC result which is shown in Figure 2. From all of the results mentioned above, we confirm that the JSC mechanism with a mixed thermal-nonthermal electron energy distribution is one possible origin of GRB 100728A GeV emission detected by *Fermi*/LAT.

The jitter/JSC calculations in this work for reproducing the multiwavelength spectrum of GRB 100728A are strongly dependent on some of the parameters mentioned above. For example, the “off-axis” parameter  $\alpha$  includes a wide range as  $0 < \alpha < \Gamma_j$ . On the other hand, as shown in Figure 2, the two observational data points have large error bars. Despite these uncertainties, some additional physical components can modify the hydrodynamics and radiative spectrum of GRB. For instance, we may further consider the gamma-ray photon annihilation as  $\gamma\gamma \rightarrow e^+e^-$  and the  $e^+e^-$  cooling as  $e^+e^- \rightarrow \gamma\gamma$ .  $\gamma\gamma$  opacity implies a minimum bulk Lorentz factor (Nakar 2007). Hascoët et al. (2011) gave a detailed study on the consequences of gamma-ray photon annihilation. Although these topics are out of the scope of our paper, we note the possibility that the jitter/JSC production has minor differences with the multi-wavelength observation.

Because the random and small-scale magnetic field can be generated by the turbulent energy spectrum ( $B^2 = \int F(k)dk$ ,  $F(k) \propto k^{-\zeta_p}$ ; see Mao & Wang 2011), in this work, we obtain  $B = 1.0 \times 10^6$  G. The cooling timescale of relativistic electrons for the radiation of jitter and JSC is  $t_{\text{cool}} = 3m_e c / 4\sigma_T \gamma (U_B + U_{\text{ph}})$ , where  $U_B$  is the energy density of magnetic field and  $U_{\text{ph}}$  is the energy density of radiation field. In the case of GRB 100728A, as  $U_B \gg U_{\text{ph}}$ , the cooling timescale is dominated by the jitter radiation:

$$t_{\text{cool}} = \frac{6\pi m_e c}{\sigma_T \gamma B^2} = 2.2 \times 10^{-8} \left( \frac{\gamma}{3.6 \times 10^4} \right)^{-1} \left( \frac{B}{1.0 \times 10^6 \text{ G}} \right)^{-2} \text{ s}, \quad (5)$$

where  $\gamma = 3.6 \times 10^4$  is the average value of the electron Lorentz factor obtained from Giannios & Spitkovsky (2009).

We use the reference value  $t_{\text{cool}} = 2.2 \times 10^{-8}$  s as the radiative cooling timescale, which is much shorter than the observed GRB duration. We expect that those fast-variability pulses shown in the GRB prompt emission/X-ray flare are produced by the extremely short-time activities of the microemitters. The gross profile (Norris et al. 2005) with a long-time duration of prompt emission/X-ray flare is the superimposing of those fast-variability pulses. We can further quantify the parameters mentioned in Section 2.2. In the shell frame, the length scale of the microemitters is

$$l_s = \gamma c t_{\text{cool}} = 2.2 \times 10^6 \left( \frac{B}{1.0 \times 10^6 \text{ G}} \right)^{-2} \text{ cm}. \quad (6)$$

The total number of microemitters within the shock shell of the thick  $\delta_s = ct_{\text{cool}}$  is

$$n = \frac{4\pi R^2 \delta_s}{l_s^3} = 7.8 \times 10^{10} \left(\frac{R}{10^{13} \text{ cm}}\right)^2 \left(\frac{\gamma}{3.6 \times 10^4}\right)^{-2} \left(\frac{B}{1.0 \times 10^6 \text{ G}}\right)^4. \quad (7)$$

The length scale of the turbulent eddy can be estimated as

$$l_{\text{eddy}} = \frac{R}{\Gamma} = 5.0 \times 10^9 \left(\frac{\alpha}{1.0}\right)^2 \left(\frac{R}{1.0 \times 10^{13} \text{ cm}}\right) \left(\frac{\Gamma_j}{100}\right)^{-1} \left(\frac{\Gamma_t}{10}\right)^{-1} \text{ cm}. \quad (8)$$

With the definition  $n_l = l_{\text{eddy}}/l_s$ , we sum up the contributions from all of the microemitters in the turbulent eddy and obtain the duration of the GRB prompt emission:

$$T = n_l n P \Gamma t_{\text{rmcool}} = 460 \left(\frac{\alpha}{1.0}\right)^4 \left(\frac{R}{1.0 \times 10^{13} \text{ cm}}\right)^3 \left(\frac{\gamma}{3.6 \times 10^4}\right)^{-3} \left(\frac{B}{1.0 \times 10^6 \text{ G}}\right)^4 \left(\frac{\Gamma_j}{100}\right)^{-2} \left(\frac{\Gamma_t}{10}\right)^{-2} \text{ s}. \quad (9)$$

This calculated timescale is roughly consistent with the observed GRB duration.

Finally, as Honda & Honda (2005) and Honda (2009) studied particle acceleration in the random and small-scale magnetic field, we adopt their result to calculate the acceleration timescale of relativistic electrons for the GRB prompt emission:

$$t_{\text{acc}} = 4.0 \times 10^{-12} \left(\frac{E}{\text{MeV}}\right)^2 \left(\frac{B}{1.0 \times 10^6 \text{ G}}\right)^{-2} \left(\frac{l_{\text{eddy}}}{5.0 \times 10^9 \text{ cm}}\right)^{-1} \left(\frac{U}{0.1c}\right)^{-2} \text{ s}, \quad (10)$$

where upstream speed is  $U \sim 0.1c$ . After comparing the cooling and acceleration timescales, and assuming  $\gamma = 3.6 \times 10^4$  and  $l_{\text{eddy}} = 5.0 \times 10^9 \text{ cm}$ , we obtain  $t_{\text{acc}} \leq t_{\text{cool}}$  below 100 MeV. This indicates that the particle acceleration is effective for the jitter mechanism.

### 3. Conclusions and Discussion

The gamma-ray emission of GRB 080319B provided evidence of the relativistic turbulent process (Kumar & Narayan 2009). It was already pointed out by Nakar & Piran (2002) that the GRB temporal profile contains many fast-variability pulses. These observational issues give us general hints into the consideration of jitter radiation in a turbulence-generated magnetic field. Using particle-in-cell (PIC) simulations, Nishikawa et al. (2009) found that a partially developed hydrodynamic-like shock structure can be created when the jet propagates into an unmagnetized plasma. The synthetic radiation spectra were also extracted from PIC simulations (Sironi & Spitkovsky 2009; Frederiksen et al. 2010). Moreover, Mizuno et al. (2011) performed relativistic magnetohydrodynamic simulations of a relativistic shock propagating through an inhomogeneous medium. It was shown that the postshock region becomes turbulent and the magnetic field is strongly amplified. In our work, the magnetic field generated by relativistic turbulence has a sub-Larmor length scale. We further

suggest that the “jet-in-jet” scenario is causing the relativistically counterstreaming plasma mentioned above.

In particular, Reynolds et al. (2010) and Reynolds & Medvedev (2011) comprehensively studied jitter radiation spectra that are dependent on the properties of anisotropic magnetic turbulence. The radiation spectra are also strongly affected by the spatial distribution of the magnetic field. In our work, the magnetic field and radiation are in the framework of the one-dimensional case. This prevents us from further investigating the topologies of the turbulent and magnetic fields in detail. However, we can compare our result and the result of Reynolds et al. (2010) and Medvedev et al. (2011) in the one-dimensional case. For example, in the study of Medvedev et al. (2011), the isotropic turbulence has the form of  $f(k) \sim k^{-2\beta}$  after the nonlinear evolution and the magnetic field is  $B^2 = f(k)$ , while it is  $B^2 = k^{\zeta_p - 1}$  in our work. Therefore, in the one-dimensional case, we obtain  $\beta = (\zeta_p - 1)/2$ . Moreover, from the study of Medvedev et al. (2011), we know that  $f(k)$  is strongly related to the topology of turbulence and the view angle  $\theta$ . The jitter parameter is given as  $K = eBl_{\text{cor}}/mc^2$ , where  $l_{\text{cor}}$  is the correlation scale, so we can clearly see that the jitter parameter is also strongly related to the topologies of the turbulent and magnetic fields.

Although the GRB emission from about 10 keV up to 10 GeV can usually be fitted by a single radiation process (see Abdo et al. 2009 for the case of GRB 080916C and Ackermann et al. 2010a for the case of GRB 090217A), sometimes an additional component is required to completely explain the GRB GeV emission. At present, GRB 090510 and GRB 100728A are two sources that have been studied by using published data sets from the simultaneous observations of *Swift* and *Fermi*. Besides GRB 100728A, GRB 090510 is another interesting source used to examine the jitter and JSC processes. *Fermi*/LAT detected the emission above 100 MeV (Ackermann et al. 2010a). De Pasquale et al. (2010) built the multiwavelength spectral energy distribution (SED) from simultaneous observations of *Swift* and *Fermi*. Synchrotron and SSC were proposed to be the origins of the keV-MeV emission and an additional component above the GeV band, respectively (Ackermann et al. 2010b), and a large bulk Lorentz factor  $\Gamma > 500 - 1000$  was required. However, it is difficult to apply the simple model presented in this paper for this burst because of two reasons. (1) A hard power-law component dominates the emission both below 20 keV and above 100 MeV (Ackermann et al. 2010b). The JSC process can be adopted to explain the emission above 100 MeV, but it cannot explain the emission below 20 keV. (2) There are no BAT data shown in the multiwavelength SED (De Pasquale et al. 2010). The spectral data in the energy range of 0.3 – 10 keV cannot well constrain the jitter slope if jitter radiation is dominated from 1 keV to 100 MeV. Moreover, it is also difficult to use the *Fermi*/LAT spectral data above 100 MeV plotted with a wide-ranging confidence interval (see the butterfly in Figure 3 of De Pasquale et al. 2010) to constrain the parameters of the JSC model.

In this paper, we use the JSC mechanism to interpret the powerful emission of GRB 100728A above the GeV band. In particular, we see two extraordinary observational behaviors of GRB 100728A. (1) A series of powerful X-ray flares (maximum rate is larger than  $500 \text{ counts s}^{-1}$ ) that occurred about 800 s after the burst trigger. (2) The significant GeV band emission was detected by *Fermi*/LAT in the same time interval as the X-ray flares. From this observational evidence, we were able to examine the jitter and JSC mechanisms. Using the jitter mechanism, we successfully reproduced prompt and X-ray emissions of GRB 100728A. To use the JSC mechanism to explain the high-energy emission of GRB 100728A above the GeV band, the jitter photons in the X-ray band should be scattered by the mixed thermal-nonthermal electrons to the GeV band. Meanwhile, the “jet-in-jet” scenario is also considered. Therefore, our model, which includes all of the main points discussed above, such as turbulence, the random and small-scale magnetic field, radiation, and geometric structure of emission, is self-consistent.

We confirm through our calculation that the jitter and JSC processes in the “jet-in-jet” scenario are valid for the multiwavelength emission of GRB 100728A without any further assumptions. However, as shown in Figure 2, the JSC result has a minor deviation to the observational data above 100 MeV. The effect of the  $\gamma\gamma$  opacity on the output spectrum is mentioned in Section 2.3. Here some other physical components are generally proposed. Although the bulk Lorentz factor of GRB jet  $\Gamma_j = 100$  and the Lorentz factor of the minijet  $\Gamma_e = 10$  are given, the shock and emission regions may have a complex structure, that can modify the radiation spectrum. The radiative efficiency is also an important issue. The relation between the cooling time of the internal shock and the shock Lorentz factor was investigated by Medvedev & Spitkovsky (2009). Moreover, instead of a constant density of shock in our case, a certain structured density profile may be involved. We speculate that the final output radiation is the superposition of multicomponent contributions.

From Figure 2, we see that the JSC radiation above the GeV band is related to the electron energy distribution. The powerful emission above the GeV band can be obtained if the seed photons are scattered by the electrons with a mixed thermal-nonthermal distribution. The weak GeV emission may have a flux value below the threshold of what an observing instrument can detect, if the seed photons are scattered by electrons with a purely nonthermal power-law distribution. In our former research (Mao & Wang 2011), the acceleration timescale is larger than the cooling timescale above 100 MeV. Thus, the jitter radiation does not work and we do not expect more GeV-GRBs. In this paper, we further explore GRB detection above the GeV band by *Fermi*/LAT that is also strongly dependent on particle acceleration. Some other interesting suggestions, such as the upscattered cocoon model (Toma et al. 2009) and the external inverse Compton model (He et al. 2011), may also be important in explaining GRB detection by *Fermi*/LAT. We hope that more multi-

wavelength data sets can be accumulated so that more penetrating studies can be performed in the future<sup>1</sup>.

We thank the referee for the instructive suggestions. This work is supported by the KASI Fellowship program, the National Natural Science Foundation of China 11173054, the National Basic Research Program of China (973 Program, 2009CB824800), and the Policy Research Program of the Chinese Academy of Sciences (KJCX2-YW-T24).

## REFERENCES

- Abdo, A. A., Ackermann, M., Ajello, M., et al. 2011, *ApJ*, 734, L27
- Abdo, A. A., Ackermann, M., Arimoto, M., et al. 2009, *Science*, 323, 1688
- Ackermann, M., Ajello, M., Baldini, L., et al. 2010a, *ApJ*, 717, L127
- Ackermann, M., Asano, K., Atwood, W. B., et al. 2010b, *ApJ*, 716, 1178
- Bregeon, J., McEnery, J., & Ohno, U. 2011, *GCN Circ.*, 12218
- Chiang, J., & Dermer, C. D. 1999, *ApJ*, 512, 699
- Corsi, A., Guetta, D., & Piro, L. 2010, *ApJ*, 720, 1008
- De Pasquale, M., Schady, P., Kuin, N. P. M., et al. 2010, *ApJ*, 709, L146
- Dermer, C. D., Chiang, J., & Mitman, K. E. 2000, *ApJ*, 537, 785
- Fan, Y. Z., Piran, T., Narayan, R., & Wei, D.-M. 2008, *MNRAS*, 384, 1483
- Frederiksen, J. T., Haugbølle, T., Medvedev, M. V., & Nordlund, Å. 2010, *ApJ*, 722, L114
- Galli, A., & Guetta, D. 2008, *A&A*, 480, 5
- Giannios, D., & Spitkovsky, A. 2009, *MNRAS*, 400, 330
- Giannios, D., Uzdebsky, D. A., & Begelman, M. C. 2010, *MNRAS*, 402, 1649

---

<sup>1</sup>The simultaneous observations of *Swift* and *Feimi*/LAT were performed on GRB 110625A (Page et al. 2011; Gruber et al. 2011; Tam & Kong 2011) and GRB 110731A (Oates et al. 2011; Bregeon et al. 2011; Gruber et al. 2011). We hope that future published data can provide more constraints on our model.

- González, M. M., Dingus, B. L., Kaneko, Y., et al. 2003, *Nature*, 424, 749
- Granot, J., & Guetta, D. 2003, *ApJ*, 598, L11
- Gruber, D., Omodei, N., Chaplin, V., et al. 2011, *GCN Circ.*, 12100
- Hascoët, R., Daigne, F., Mochkovitch, R., & Vennin, V. 2011, *MNRAS*, arXiv: 1107.5737
- He, H.-N., Zhang, B.-B., Wang, X.-Y., Li, Z., & Mészáros, P. 2011, arXiv: 1112.2253
- Honda, M. 2009, *ApJ*, 706, 1517
- Honda, M., & Honda, Y. S. 2005, *ApJ*, 633, 733
- Hurley, K., Dingus, B. L., Mukherjee, R., et al. 1994, *Nature*, 372, 652
- Katarzyński, K., Ghisellini, G., Mastichiadis, A., Tavecchio, F., & Maraschi, L. 2006, *A&A*, 453, 47
- Kirk, J. G., & Reville, B. 2010, *ApJ*, 710, L6
- Kumar, P., & Narayan, R. 2009, *MNRAS*, 395, 472
- Lazar, A., Nakar, E., & Piran, T. 2009, *ApJ*, 695, L10
- Lyutikov, M. 2006, *MNRAS*, 369, L5
- Mao, J., & Wang, J. 2007, *ApJ*, 669, L13
- Mao, J., & Wang, J. 2011, *ApJ*, 731, 26
- Medvedev, M. V. 2000, *ApJ*, 540, 704
- Medvedev, M. V. 2006, *ApJ*, 637, 869
- Medvedev, M. V., Frederiksen, J. T., Haugbølle, T., Nordlund, Å. 2011, *ApJ*, 737, 55
- Medvedev, M. V., & Loeb, A. 1999, *ApJ*, 526, 697
- Medvedev, M. V., & Spitkovsky, A. 2009, *ApJ*, 700, 956
- Mészáros, P., Laguna, P., & Rees, M. J. 1993, *ApJ*, 415, 181
- Mészáros, P., Rees, M. J., & Papathanassiou, H. 1994, *ApJ*, 432, 181
- Mizuno, Y., Pohl, M., Zhang, B., Nishikawa, K.-I., & Hardee, P. E. 2011, *ApJ*, 726, 62

- Nakar, E. 2007, *Phys. Rep.*, 442, 166
- Nakar, E., & Piran, T. 2002, *MNRAS*, 331, 40
- Narayan, R., & Kumar, P. 2009, *MNRAS*, 394, L117
- Nishikawa, K.-I., Niemić, J., Hardee, P. E., et al. 2009, *ApJ*, 698, L10
- Norris, J. P., Bonnell, J. T., Kazanas, D., et al. 2005, *ApJ*, 627, 324
- Oates, S. R., Beardmore, A. P., Holland, S. T., et al. 2011, *GCN Circ.*, 12215
- Page, K. L., Barthelmy, S. D., Beardmore, A. P., et al. 2011, *GCN Circ.*, 12088
- Reynolds, S. J., & Medvedev, M. V. 2011, arXiv: 1106.4879
- Reynolds, S. J., Pothapragada, S., & Medvedev, M. V. 2010, *ApJ*, 713, 764
- Rybicki, G., & Lightman, A. P., 1979, *Radiative Processes in Astrophysics* (New York: Wiley Interscience)
- Schekochihin, A. A., Cowley, S. C., Tayler, S. F., Marson, J. A., & McWilliams, J. C. 2004, *ApJ*, 612, 276
- Schlickeiser, R. 1989a, *ApJ*, 336, 243
- Schlickeiser, R. 1989b, *ApJ*, 336, 264
- She, Z.-S., & Leveque, E. 1994, *Phys. Rev. Lett.*, 72, 336
- Sironi, L., & Spitkovsky, A. 2009, *ApJ*, 707, L92
- Stawarz, L., & Petrosian, V. 2008, *ApJ*, 681, 1725
- Tam, P. H. T., & Kong, A. K. H. 2011, *GCN Circ.*, 12097
- Toma, K., Wu, X.-F., & Mészáros, P. 2009, *ApJ*, 707, 1404
- Wang, X. Y., Dai, Z. G., & Lu, T. 2001, *ApJ*, 546, L33
- Wang, X. Y., Li, Z., & Mészáros, P. 2006, *ApJ*, 641, 89
- Zhang, B., & Mészáros, P. 2001, *ApJ*, 559, 110
- Zou, Y. C., Fan, Y. Z., & Piran, T. 2009, *MNRAS*, 396, 1193

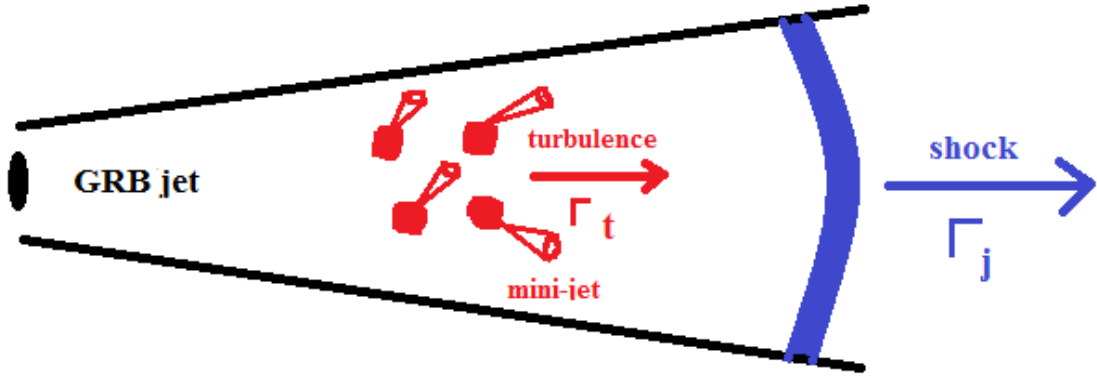


Fig. 1.— Illustration of the “jet-in-jet” scenario. The turbulent process occurs after shock propagation. The bulk Lorentz factor of the GRB jet is  $\Gamma_j$ . The microemitter with its minijet has the Lorentz factor  $\Gamma_e$ , and  $\Gamma_e \sim \Gamma_t$ , where  $\Gamma_t$  is the Lorentz factor of turbulence.

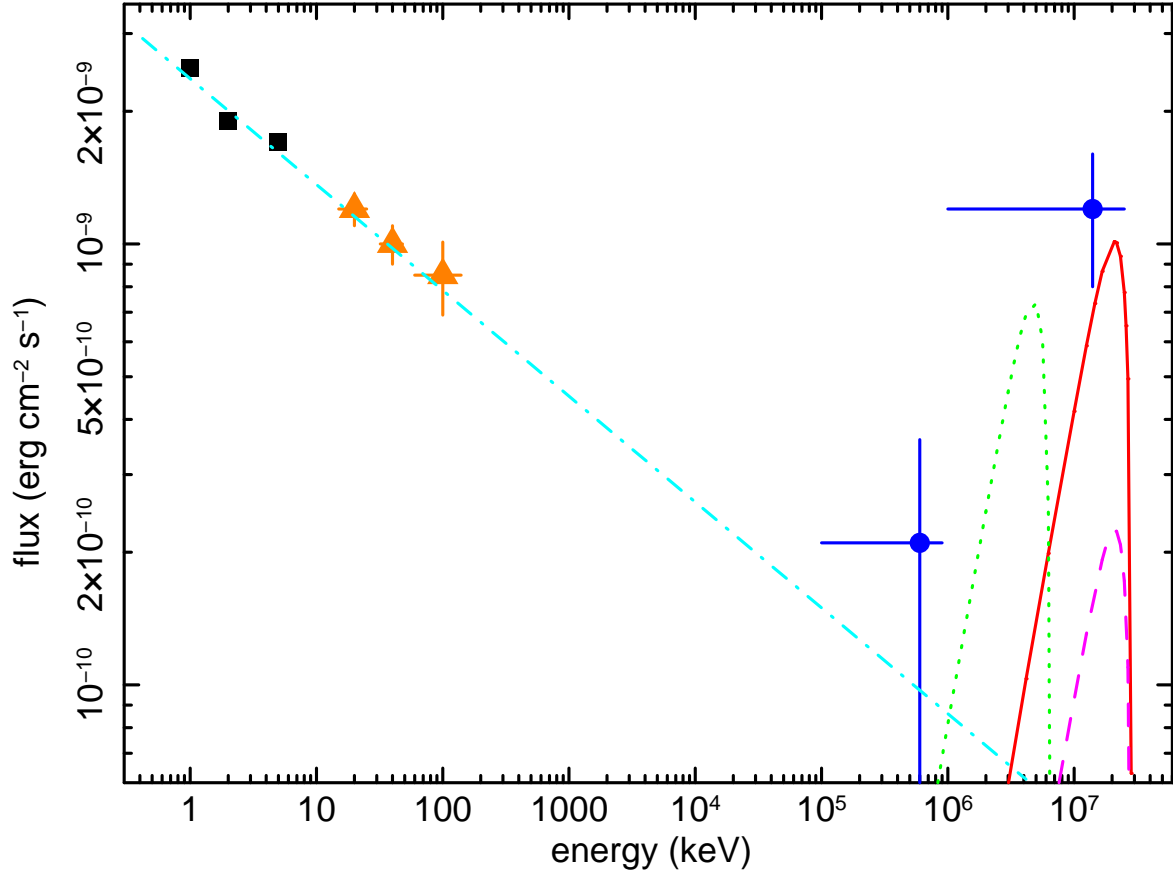


Fig. 2.— Jitter and JSC radiation of GRB 100728A. The observational data from Abdo et al. (2011) are denoted by solid squares (XRT data), solid triangles (BAT data), and solid circles (LAT data). The result of jitter radiation with the spectral slope 0.24 is denoted by a dash-dotted line. The JSC results calculated using a mixed thermal-nonthermal electron energy distribution (given by Equations (3) & (4)) are shown: a solid line denotes the JSC result in the case of  $\gamma_{\max} = 10^6$  and a dotted line denotes the JSC result in the case of  $\gamma_{\max} = 5 \times 10^5$ . For comparison, the JSC result calculated using a power-law electron energy distribution ( $\gamma_{\min} = \gamma_{\text{nth}} = 10^3, \gamma_{\max} = 10^6$ ) is denoted by a dashed line.